九州大学大学院総合理工学報告
第30巻　第2号　307-312頁　平成20年9月

Engineering Sciences Reports, Kyushu University
Vol. 30, No. 2, pp. 307-312, SEP. 2008

Rotation of Ethylene Molecule on the Organometallic Species: A Possibility to Control the Rotation Rate

Hideo KONDO*3 Taizo HAYASHIDA*4 Yoshitaka YAMAGUCHI*4
Yusuke SUNADA*1, 2 and Hideo NAGASHIMA*1, 2†
†E-mail of corresponding author: *nagasima@cm.kyushu-u.ac.jp*

(Received July 31, 2008)

Coordination behavior of ethylene on the cationic or neutral ruthenium amidinate species was studied by combination of spectroscopy and molecular orbital considerations. The result suggests that the rotation rate of coordinated ethylene is dependent on the donor property of the ruthenium counterpart, and can be controlled by appropriate choice of the auxiliary ligands.

Key words: *Ethylene, Rotation, Ruthenium, Amidinate, Donor property, Variable temperature NMR study, σ-donation, π-back donation*

1. Introduction

Molecular machines are one of the ultimate device in the next generation; however, there require a number of fresh idea to realize them. We consider that fundamental research on the dynamic behavior of the moloecules may be a clue to obtain the new concept for molecular machine. The content of this paper is basic research on the dynamic behavior of ethylene molecule coordinated to organometallic species in solution, which can be detected by Nuclear Magnetic Resonance Spectroscopy (NMR) in solution states. Coordination of ethylene to the metal is governed by molecular orbitals, in which two factors, correlations of HOMO of ethylene with empty orbitals of metal (donation) and that of LUMO with occupied orbitals of metal (back donation) are important.[1)] As reported in detail in MO diagrams in the literature,[2)] the coordinated ethylene molecule freely rotates when the donation is a major factor for the coordination. In contrast, strong back donation retards the rotation. Since proportion of donation to back donation is dependent on the electronic property of the organometallic species, the rate of the rotation of ethylene on the metallic species, fast or slow, varied with the ligands of the metallic species bonded with ethylene as shown in Fig.1. We describe here that coordinatively unsaturated ruthenium amidinate complexes react with ethylene to form the corresponding ethylene complexes, on which the coordinated ethylene rotates in the coordination sphere. It is important that we successfully realized the fast and slow rotation of the ethylene ligand on the ruthenium atom, which was achieved by appropriate change of the electronic property of the organoruthenuim counterpart (Fig 2).

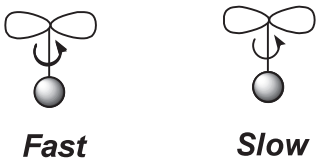

Fig.1 Rotation of ethylene on the metallic species.

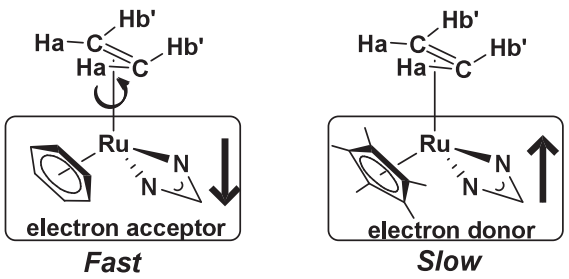

Fig.2 Rotation of ethylene on the organoruthenium fragment.

*1 Institute for Materials Chemistry and Engineering
*2 Department of Molecular and Material Sciences
*3 Department of Molecular and Material Sciences, Ph.D student
*4 Department of Molecular and Material Sciences, Graduate Student

2. Results and Discussion

2.1 Synthesis and dynamic behavior of η^2-ethylene complexes of ruthenium amidinates bearing the η^6-C_6H_6 or η^5-C_5Me_5 ligand

Treatment of a cationic 16 electron ruthenium amidinate bearing a benzene ring, [(η^6-C_6H_6)Ru(η^2-^{t}BuN=C(Ph)N^{t}Bu)](TFPB) (**1**) [TFPB = $^-$B{3,5-$(CF_3)_2C_6H_3$}$_4$], with ethylene in CH_2Cl_2 at room temperature instantly gave [(η^6-C_6H_6)Ru(η^2-H_2C=CH_2)(η^2-^{t}BuN=C(Ph)N^{t}Bu)](TFPB) (**2**) in quantitative yield (Scheme 1).

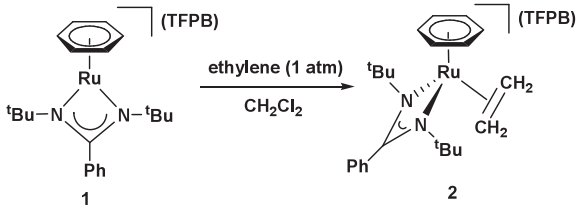

Scheme 1

The molecular structure of [(η^6-C_6H_6)Ru(η^2-H_2C=CH_2)(η^2-^{t}BuN=C(Ph)N^{t}Bu)](TFPB) (**2**) determined by X-ray diffraction analysis is depicted in Fig. 3. The ruthenium center adopts a three legged piano stool structure with two nitrogen atom of the amidinate ligand and the centroid of the η^2-coordinated ethylene moiety. The ethylene moiety is bound to the ruthenium center parallel to the η^6-C_6H_6 ring.

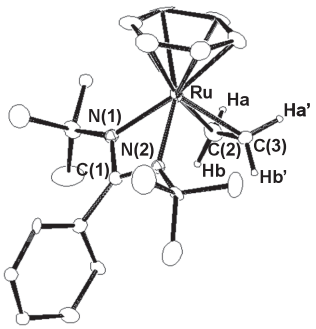

Fig.3 Molecular structure of **2** showing 30 % probability ellipsoids. Hydrogen atoms and counter anion (TFPB) were omitted for clarity.

Although the crystal structure shows that ethylene is coordinated to the ruthenium atom parallel to the benzene ring, variable temperature NMR spectra are inconsistent with those deduced from the molecular structure. According to the crystal structure of **2**, two protons of the ethylene ligand (Ha and Ha') close to the benzene are magnetically equivalent, but inequivalent to the other set of equivalent protons, Hb, Hb'. In the actual ^{1}H NMR spectrum at room temperature, only a singlet appeared at 4.3 ppm, which is apparently different from non-coordinated ethylene (5.4 ppm).[3] This singlet starts to broaden at -60 °C, and disappeared at -80 and -100 °C (Fig. 4). If the crystal structure corresponds to the ^{1}H NMR spectra, the coordinated ethylene should give two doublets, which are observed in the NMR spectra of **4** at low temperature (vide infra). The reasonable interpretation of the NMR spectra is that the ethylene ligand in **2** is freely rotated in the NMR time scale up to -100 °C.

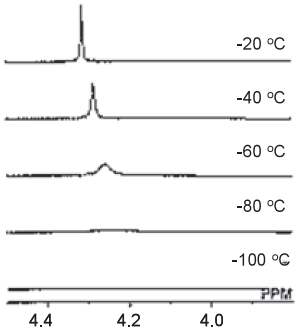

Fig.4 Variable temperature ^{1}H NMR signals for coordinated ethylene protons of **2**.

An isoelectronic neutral analogue of **2** was synthesized by treatment of (η^5-C_5Me_5)Ru(η^2-^{t}BuN=C(Ph)N^{t}Bu) (**3**) with ethylene in THF at room temperature (Scheme 2).[4] Variable temperature ^{1}H NMR studies on **4** revealed that two doublets was observed at -90 °C, coalesced at -45 °C, and became a singlet at 2.68 ppm at room temperature (Fig. 5). Deduced from the molecular structure of analogous compounds, **4** has a similar skeleton to **2**. The spectra below -60 °C suggest that the slow rotation of the ethylene ligand in **4** in the NMR time scale; it is slow enough to show that two protons, Ha and Ha', close to the η^5-C_5Me_5 ligand appears inequivalent to the other two, Hb and Hb'.

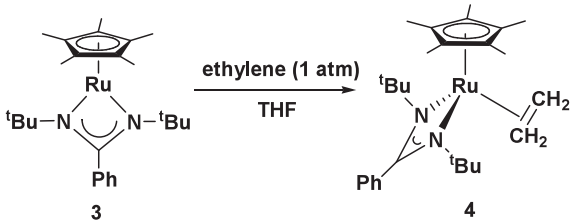

Scheme 2

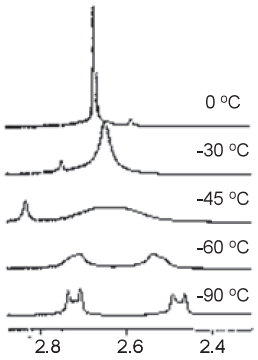

Fig.5 Variable temperature ^{1}H NMR signals for coordinated ethylene protons of **4**.

2.2 Considerations on the dynamic behavior of 2 and 4

Although the above described ethylene comlexes are isoelectronic, the rotation rate is apparently in the order, **2** > **4**. EHMO calculations provides a clue for qualitative understanding the rate difference. The bonding interaction between the ruthenium amidinate fragment (η^5-C_5H_5)Ru(η^2-HN-CH=NH) or (η^6-C_6H_6)Ru$^+$(η^2-HN-CH=NH) with ethylene as the model of the complex **1** or **3** is illustrated in Fig. 6. In both of the cases, the important correlation is seen in HOMO of ethylene (π) with the vacant d_{xz} orbital of the metal fragment (σ-donation), and the occupied d_{yz} orbital of the

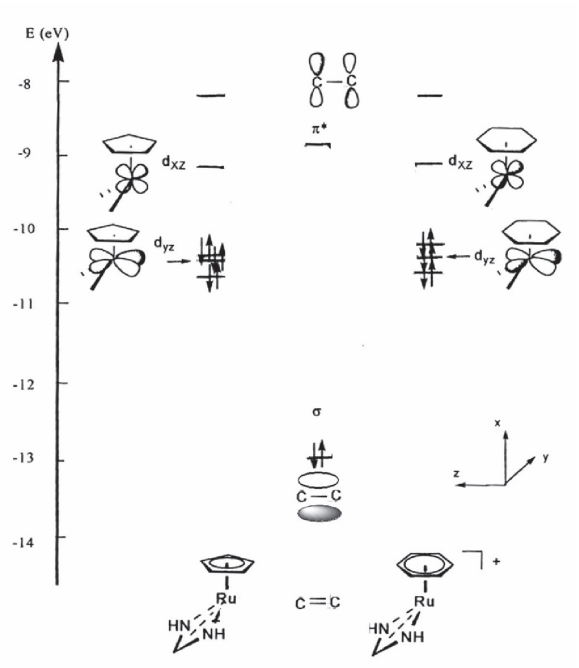

Fig.6 The interaction diagram between ethylene and (η^5-C_5H_5)Ru(η^2-HN-CH=NH) or (η^6-C_6H_6)Ru(η^2-HN-CH=NH).

metal fragment with the LUMO (π^*) of ethylene (π-back donation). As shown in Fig. 7, rotation of $\pi \rightarrow d_{xz}$ interaction along with the axis does not give a mismatch of orbital symmetry, whereas that of $d_{yz} \rightarrow \pi^*$ interaction is not allowed due to significant decrease of overlapping of the orbitals.

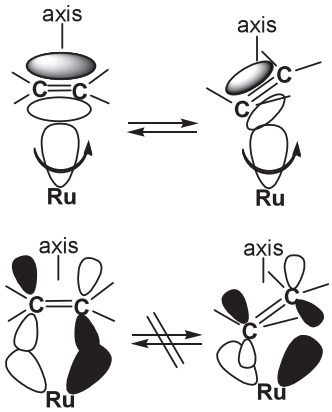

Fig.7 The overlapping of the molecular orbitals for (a) σ-donation (upper) and (b) π-back donation (lower)

A problem is how to explain the difference in the rotational barrier observed between **2** and **4**. EHMO calculations are not accurate enough to discuss the quantitative difference in energy of the metal fragment. In fact, energy of (η^5-C_5H_5)Ru(η^2-HN-CH=NH) is the same as that of (η^6-C_6H_6)Ru$^+$(η^2-HN-CH=NH) in the EHMO level. For quantitative consideration, we were interested in the CO complexes of ruthenium amidinates. As shown in Fig. 8, σ-donation is established by $\sigma \rightarrow d_{xz}$ interaction, whereas π-back donation is done by $d_{yz} \rightarrow \pi^*$ interaction. Proportion of σ-donation to π-back donation affects the bond order of the CO ligand; strong σ-donation enhances the nature of C-O triple bond, whereas strong π-back donation reduces the C-O bond order. These are estimated by ν_{CO} absorptions on the IR spectrum.[5]

Fig.8 Bonding mode of CO. σ-donation (left) and π-back donation (right).

The CO adduct of **1** was readily prepared by the reaction of **1** with CO (1 atm) in CH_2Cl_2 within 5 min (Scheme 3). Similarly, an analogous neutral η^1-CO complex was synthesized by the reaction of **3** with 1 atm of CO as

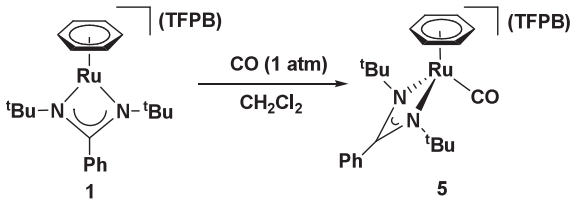

Scheme 3

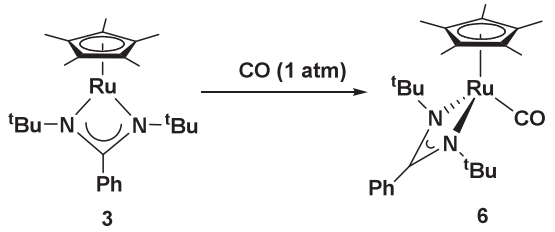

Scheme 4

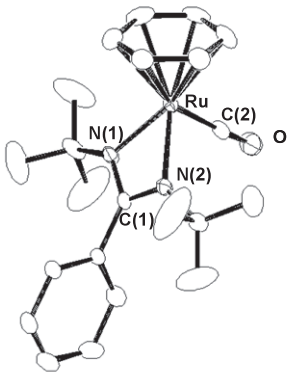

Fig.9 Variable temperature ^{1}H NMR signals for coordinated ethylene protons of **4**.

briefly reported in our previous paper (Scheme 4).[6] The molecular structure of **5** was determined by crystallography as shown in Fig. 9. The ruthenium center adopts a three legged piano stool structure with two nitrogen atom of the amidinate ligand and the carbon atom of the CO moiety. The CO ligand is bound to the ruthenium center in a η^1- fashion, and the bond distance (1.149(10) Å) is in the range of normal coordinatively saturated η^1-CO complexes.

The IR spectrum of **5** is characteristic in giving C≡O stretching bands at 2050 cm^{-1}. In contrast, that of **6** showed a strong ν_{CO} absorption band at 1888 cm^{-1}, which is lower by ca. 150 cm^{-1} than that of **5**. The lower ν_{CO} means the lower bond order of C-O and strong π-back donation. This clearly suggests that the $(\eta^5\text{-}C_5Me_5)Ru(\eta^{2}\text{-}^{t}BuN{=}C(Ph)N^{t}Bu)$ fragment is a better donor than the $(\eta^6\text{-}C_6H_6)Ru^{+}(\eta^{2}\text{-}^{t}BuN{=}C(Ph)N^{t}Bu)$. [7] In other words, interaction of ethylene with $(\eta^5\text{-}C_5Me_5)Ru(\eta^{2}\text{-}^{t}BuN{=}C(Ph)N^{t}Bu)$ fragment having a higher lying HOMO is governed by π-back donation, $d_{yz}\rightarrow\pi^*$; this is not favorable for the rotation of the ethylene ligand as described above. In contrast, a major contribution of σ-donation, $p\rightarrow d_{xz}$, in the interaction of ethylene with the better electron acceptor $(\eta^6\text{-}C_6H_6)Ru^{+}(\eta^{2}\text{-}^{t}BuN{=}C(Ph)N^{t}Bu)$ fragment having lower lying LUMO does not prevent rotation of ethylene on the metal fragment.

3. Summary and Conclusion

Coordination of ethylene to metal species has long been investigated both experimentally and theoretically. Famous Dewar-Chatt-Dunkanson model is the first illustration of the metal-ethylene bonding based on the molecular orbitals.[1] Earlier work by Hoffman and coworkers showed that EHMO calculations are useful for understanding semi-quantitive discussion on the coordination behavior of ethylene.[2] Isolable coordinatively unsaturated complexes are advantageous on the point that electronic property can be varied with the auxiliary ligands. Experimental studies on the coordination behavior of ethylene to the coordinativeluy unsaturated complexes are attractive; however, investigation in this line is rare compared with the coordination behavior of CO. The present study using two isoelectronic ruthenium complexes is a rare example showing that the rotational barrier of ethylene on the metal is dependent on the electronic property of the metal fragment.

4. Experiment

4.1 General

Manipulation of air and moisture sensitive organometallic compounds was carried out under a dry argon atmosphere using standard Schlenk tube techniques associated with a high-vacuum line, or with the nitrogen filled glove box. All solvents were distilled over appropriate drying reagents prior to use (THF, pentane; Ph_2CO/Na, C_6H_5F, CH_2Cl_2; CaH_2). ^{1}H, ^{13}C, ^{31}P NMR spectra were recorded on a JEOL Lambda 600 or a Lambda 400 spectrometer at ambient temperature unless otherwise noted. ^{1}H and ^{13}C chemical shifts (δ values) were given in ppm relative to the solvent signal. IR spectra were recorded in cm^{-1} on a JASCO FT/IR-550 spectrometer. Melting points were measured on a Yanaco SMP3 micro melting point apparatus. Elemental analyses were performed by the Elemental Analysis Center, Faculty of Science, Kyushu University. Starting materials, $[(\eta^5\text{-}C_5Me_5)RuCl]_4$ [8], $[(arene)RuCl_2]_2$ [9], and complex **1**, **3**, and **6** [4, 6],

were synthesized by the method reported in the literature.

4.2 Experimental results

4.2.1 Synthesis of [(η^6-C_6H_6)Ru(η^2-H_2C=CH_2)(η^2-^{t}BuN=C(Ph)N^{t}Bu)](TFPB) (2)

In a Schlenk tube, [(η^6-C_6H_6)Ru(η^2-^{t}BuN=C(Ph)N^{t}Bu)](TFPB) (62 mg, 0.05 mmol) was dissolved in CH_2Cl_2 (2 mL) and cooled to -78 °C. Then 1 atm of ethylene was introduced, and the reaction mixture was stirred at room temperature for 5 min. The color of the reaction mixture was immediately changed from violet to brown. This solution was layered with n-pentane and cooled to -35 °C, from which dark brown crystals of **2** was obtained in 60 % yield. Mp: 100 °C (dec). ^{1}H NMR (CD_2Cl_2, 400 MHz, -20 °C) δ 0.96 (s, 18H, C(CH_3)$_3$), 4.31 (s, 4H, H_2C=CH_2), 6.16 (s, 6H, C_6H_6), 6.96 - 6.98 (m, 1H, Ph), 7.18 - 7.19 (m, 1H, Ph), 7.24 - 7.26 (m, 1H, Ph), 7.34 - 7.36 (m, 1H, Ph), 7.40 - 7.44 (m, 1H, Ph), 7.55 (s, 4H, (CF_3)$_2$$C_6H_3$), 7.71 (s, 8H, ($CF_3$)$_2$$C_6H_3$). ^{13}C NMR ($CD_2Cl_2$, 150 MHz, -20 °C) δ 32.8 (C(*C*H$_3$)$_3$), 55.7 (*C*(CH$_3$)$_3$), 70.0 (s, H_2*C*=*C*H_2), 92.0 (s, *C*$_6$H$_6$), 116.7 - 117.1 (m, (CF_3)$_2$*C*$_6$H$_3$), 123.8 (q, $J_{C\text{-}F}$ = 272.6 Hz, CF_3),126.8 (s, Ph), 127.2 (s, Ph), 128.1 (q, $J_{C\text{-}F}$ = 28.5 Hz, (CF_3)$_2$*C*$_6$H$_3$), 128.7 (s, Ph), 129.4 (s, Ph), 130.3 (s, Ph), 133.9 - 134.2 (m, (CF_3)$_2$*C*$_6$H$_3$), 136.6 (s, Ph), 161.1 (q, $J_{C\text{-}B}$ = 49.9 Hz, (CF_3)$_2$*C*$_6$H$_3$), 172.6 (s, NCN).

4.2.2 Synthesis of (η^5-C_5Me_5)Ru(η^2-H_2C=CH_2)(η^2-^{t}Bu-N=C(Ph)N^{t}Bu) (4)

In a NMR tube, (η^5-C_5Me_5)Ru(η^2-^{t}BuN=C(Ph)N^{t}Bu) (48 mg, 0.01 mmol) was dissolved in THF-d_8 (0.5 mL). Then 1 atm of ethylene was introduced, and the reaction mixture was shaken by hand for 5 min. The color of the reaction mixture was immediately changed from violet to yellow, and quantitative formation of **4** was confirmed by ^{1}H NMR spectrum. ^{1}H NMR (THF-d_8, 600 MHz, r.t.) δ 0.96 (s, 18H, C(CH_3)$_3$), 1.58 (s, 15H, C_5(CH_3)$_5$), 2.68 (s, 4H, H_2C=CH_2), 7.12 - 7.27 (m, 5H, Ph). ^{13}C NMR (THF-d_8, 150 MHz, r.t.) δ 10.7 (C_5*Me*$_5$), 35.9 (C(*C*H$_3$)$_3$), 44.4 (s, H_2*C*=*C*H_2), 54.2 (*C*(CH$_3$)$_3$), 89.8 (*C*$_5$Me$_5$), 127.0 (s, Ph), 127.3 (s, Ph), 128.5 (s, Ph), 132.3 (s, Ph), 134.3 (s, Ph), 141.8 (s, Ph), 167.5 (s, NCN).

4.2.3 Synthesis of [(η^6-C_6H_6)Ru(η^1-CO)(η^2-^{t}Bu-N=C(Ph)N^{t}Bu)](TFPB) (5)

In a Schlenk tube, [(η^6-C_6H_6)Ru(η^2-^{t}BuN=C(Ph)N^{t}Bu)](TFPB) (52 mg, 0.04 mmol) was dissolved in CH_2Cl_2 (3 mL) and cooled to -78 °C. Then 1 atm of CO gas was introduced, and the reaction mixture was stirred at room temperature for 5 min. The color of the reaction mixture was gradually changed from violet to orange-red. The solvent was removed under vaccum, then recrystallization from CH_2Cl_2/pentane at -35 °C gave orange-red crystals of **5** in 90 % yield (48 mg, 0.037 mmol). m.p.: 150 °C (dec). Anal. Calcd for $C_{54}H_{41}N_2OBF_{24}Ru$: C, 49.82; H, 3.17; N, 2.15. Found: C, 49.59; H, 3.17; N, 2.19. IR (KBr, pellet): ν_{CO}(cm^{-1}) = 2050 (s). ^{1}H NMR (CD_2Cl_2, 400 MHz, r.t.) δ 0.90 (s, 18H, C(CH_3)$_3$), 6.21 (s, 6H, C_6H_6), 7.08 - 7.10 (m, 1H, Ph), 7.14 - 7.16 (m, 1H, Ph), 7.31 - 7.41 (m, 2H, Ph), 7.46 - 7.48 (m, 1H, Ph), 7.54 (s, 4H, (CF_3)$_2$$C_6H_3$), 7.71 (s, 8H, ($CF_3$)$_2$$C_6H_3$). ^{13}C NMR ($CD_2Cl_2$, 100 MHz, r.t.) δ 32.8 (C(*C*H$_3$)$_3$), 56.8 (*C*(CH$_3$)$_3$), 96.6 (s, *C*$_6$H$_6$), 117.4 - 117.7 (m, (CF_3)$_2$*C*$_6$H$_3$), 124.5(q, $J_{C\text{-}F}$ = 272.4 Hz, CF_3), 127.8 (s, Ph), 128.4 (s, Ph), 128.7 (s, Ph), 129.5 (s, Ph), 128.7 - 129.2 (m, (CF_3)$_2$*C*$_6$H$_3$), 130.3 (s, Ph), 134.6 - 135.0 (m, (CF_3)$_2$*C*$_6$H$_3$), 136.6 (s, Ph), 161.7 (q, $J_{C\text{-}B}$ = 51.1 Hz, (CF_3)$_2$*C*$_6$H$_3$), 178.3 (s, NCN), 191.8 (s, CO).

4.2.4 X-ray data collection and reduction

X-ray crystallography was performed on a Rigaku RAXIS RAPID imaging plate diffraction meter with graphite monochromated Mo-Kα radiation (λ = 0.71070A). The data were collected at 223(2) K. The data were corrected for Lorentz and polarization effects. The structures were solved, by direct method (SIR92) [10] for **2**, by Patterson method (DIRDIF94 PATTY) [11] for **5**, and expanded using Fourier techniques [12]. The non-hydrogen atoms were refined anisotropically. Hydrogen atoms were refined using the riding model. The final cycle of full-matrix least-squares refinement on F^2 was based on 4598 observed reflections and 822 variable parameters for **2**, 6272 observed reflections and 1117 variable parameters for **5**. Neutral atom scattering factors were taken from Cromer and Waber. [13] All calculations were performed using the teXsan [14] crystallographic software package of Molecular Structure Corporation except for refinement, which was performed using SHELXL-97 [15]. Details of final refinement are summarized in Table 1, and the numbering scheme employed is shown in Fig. 5 and 9, which was drawn with ORTEP at 30% probability ellipsoid.

Table 1 Crystal data and parameters for **2** and **5**

complex	**2**	**5**
Empirical Formula	$C_{55}H_{44}N_2BF_{24}Ru$	$C_{54}H_{41}N_2OBF_{24}Ru$
Formula Weight	1300.81	1301.77
Crystal Color, Habit	Brown, prism	Red, block
Crystal Dimensions, mm	0.14 x 0.13 x 0.07	0.23 x 0.18 x 0.16
Crystal System	Triclinic	Triclinic
Lattice Type	Primitive	Primitive
a, Å	15.232(1)	12.2994(10)
b, Å	17.1464(6)	15.1197(10)
c, Å	12.1591(3)	17.0319(10)
α, deg	107.908(1)	71.736(5)
β, deg	91.200(2)	72.111(6)
γ, deg	71.313(2)	89.142(5)
V, Å^3	2851.8(2)	2850.7(4)
Space Group	P-1 (#2)	P-1 (#2)
Z value	2	2
Dcalc, g/cm^3	1.515	1.516
F_{000}	1306.00	1304.00
μ(MoKα)	3.91 cm^{-1}	3.93 cm^{-1}
$2\theta_{max}$	55.0°	54.9°
Radiation	MoKα (λ = 0.71070 Å)	
no. of rflns measd	12451	13636
no. of unique rflns	4598	6272
Residuals: R1 (I>2.00σ(I))	0.113	0.071
Residuals: wR2 (All reflections)	0.287	0.076
Goodness of Fit Indicator	1.300	4.04
Max Shift/Error in Final Cycle	0.000	0.000
Maximum peak in Final Diff. Map	0.51 e$^-$/Å^3	0.75 e$^-$/Å^3
Minimum peak in Final Diff. Map	-0.51 e$^-$/Å^3	-0.64 e$^-$/Å^3

Acknowledgments

This work was partly supported by a Grant-in-Aid for Scientific Research from the Ministry of Education, Culture, Sports, Science and Technology, Japan.

References

1) (a) M. J. S. Dewar, *Bull. Soc. Chim. Fr.* **18**, C79 (1951). (b) J. Chatt, L. A. Duncanson, *J. Chem. Soc.* 2939 (1953).
2) For a review; (a) G. Frenking, N. Fröhlich, *Chem. Rev.* **100**, 717 (2000) and reference therein. Typical examples, see; (b) T. A. Albright, R. Hoffmann, J. C. Thibeault, D. L.Thorn, *J. Am. Chem. Soc.* **101,** 3801 (1979).
3) (a) H. V. R. Dias, J. Wu, *Eur. J. Inorg. Chem.* 509 - 522 (2008). (b) H. V. R. Dias, J. Wu, *Eur. J. Inorg. Chem.* 509 - 522 (2008). (c) J. A. Flores, H. V. R. Dias, *Inorg. Chem.* **47**, 4448 (2008).
4) (a) T. Hayashida, Y. Yamaguchi, K. Kirchner, H. Nagashima, *Chem. Lett.* **30**, 954 (2001). (b) For an account; H. Nagashima, H. Kondo, T. Hayashida, Y. Yamaguchi, M. Gondo, S. Masuda, K. Miyazaki, K. Matsubara, K. Kirchner, *Coord. Chem. Rev.* **245**, 177 (2003).
5) Caulton et al. have described the synthesis of several coordinatively unsaturated ruthenium complexes of the type (η^5-C_5Me_5)RuLX (L = P^iPr_2Ph, PCy_3; X = Cl, Br, I, OCH_2CF_3, $OSiPh_3$, $OSiMe_2Ph$, NHPh), which readily react with small molecules such as CO and ethylene. They also described that the $\nu_{C\equiv O}$ value in the IR spectrum of η^1-CO complexes is the good indicator to clarify the electron density around the metal center. See T. J. Johnson, K. Folting, W. E. Streib, J. D. Martin, J. C. Huffman, S. A. Jackson, O. Eisenstein, K. G. Caulton, *Inorg. Chem.* **34**, 488 (1995).
6) Y. Yamaguchi, H. Nagashima, *Organometallics* **19**, 725 (2000).
7) The significantly low-filed shifted ^{1}H and ^{13}C NMR siganls of ethylene moiety in **2** compared with **4** are another sign for weak back donation. As the back-donation to the antibonding orbital of ethylene increased, the hybridization of the ethylene moiety should be changed from sp^2 to sp^3, leading to high-field shift in the NMR spectrum.
8) P. J. Fagan, M. D. Ward, J. C. Calabrese, *J. Am. Chem. Soc.* **111**, 1698 (1989).
9) M. A. Bennet, A. K. Smith, *J. Chem. Soc., Dalton Trans.* 233 (1974)
10) SIR92; A. Altomare, M. Cascarano, C. Giacovazzo, A. Guagliardi, *J. Appl. Cryst.* **26**, 343 (1993).
11) DIRDIF94; P. T. Beurskens,G. Admiraal, G. Beurskens, W. P. Bosman, S. Garcia-Granda, R. O. Gould, J. M. M. Smits, C. Smykalla, The DIRDIF-94 program system; *Technical Report of the Crystallography Laboratory*; University of Nijmegen, Nijmegen, The Netherlands (1992).
12) PATTY; P. T. Beurskens, G. Admiraal, G. Beurskens, W. P. Bosman, S. Garcia-Granda, R. O. Gould, J. M. M. Smits, C. Smykalla, The DIRDIF program system; *Technical Report of the Crystallography Laboratory*; University of Nijmegen, Nijmegen, The Netherlands (1992).
13) D. T. Cromer, J. T. Waber, *International Tables for X-ray Crystallography*; Kynoch Press; Birmingham, U.K., 1974 *Vol. 4.*
14) teXsan for Windows; Crystal Structure Analysis Package, Molecular Structure Corporation (1997).
15) SHELX97; G. M. Sheldrick (1997).